Oxidation Chemistry of (−)-Norepinephrine in the Presence of L-Cysteine

Xue-Ming Shen and Glenn Dryhurst*

Department of Chemistry and Biochemistry, University of Oklahoma, Norman, Oklahoma 73019

Received January 5, 1996[⊗]

The noradrenergic neurotransmitter (−)-norepinephrine (**1**) is very easily oxidized at physiological pH to an *o*-quinone (**2**) that normally cyclizes and subsequently oxidatively polymerizes to black melanin. In this investigation it is demonstrated that L-cysteine (CySH) can divert the melanin pathway by efficiently scavenging *o*-quinone **2** to give, initially, 5-*S*-cysteinylnorepinephrine (**6**) and 2-*S*-cysteinylnorepinephrine (**7**). These cysteinyl conjugates are appreciably more easily oxidized than **1** to *o*-quinones that, in part, are further attacked by CySH to give 2,5-bi-*S*-cysteinylnorepinephrine (**8**), an even more easily oxidized compound. The *o*-quinone intermediates formed upon oxidation of **6**−**8** can also undergo facile intramolecular cyclizations to bicyclic *o*-quinone imines that oxidize the cysteinyl conjugates from which they are derived in a reaction sequence that leads initially to a number of dihydrobenzothiazines. At least two of these compounds, 7-(1-hydroxy-2-aminoethyl)-3,4-dihydro-5-hydroxy-2*H*-1,4-benzothiazine-3-carboxylic acid (**9**) and 8-(1-hydroxy-2-aminoethyl)-3,4-dihydro-5-hydroxy-2*H*-1,4-benzothiazine-3-carboxylic acid (**10**) are lethal when administered into the brains of mice. The *in vitro* chemical pathways elucidated in this investigation might be of relevance to the depigmentation and degeneration of neuromelanin-pigmented noradrenergic cell bodies in the locus ceruleus in Parkinson's Disease and to the degeneration of noradrenergic nerve terminals in Alzheimer's Disease and following transient cerebral ischemia (stroke).

The primary neuropathological feature of Parkinson's Disease (PD) is the profound degeneration of nigrostriatal dopaminergic neurons caused by toxic processes that occur in their pigmented cell bodies in the substantia nigra (SN).[1,2] Dopaminergic SN cells are pigmented as a result of the autoxidation of cytoplasmic dopamine (DA) to DA-*o*-quinone that polymerizes to black neuromelanin.[3,4] The pathological processes that occurs in these neurons include oxidative stress[5] and a defect in mitochondrial respiration[6] although the underlying mechanisms are unknown. However, the Parkinsonian SN is characterized by a massive loss of glutathione (GSH) without a corresponding increase in GSSG,[5,7,8] an increased 5-*S*-cysteinyldopamine (5-*S*-CyS-DA)/DA concentration ratio,[9] increased γ-glutamyl transpeptidase (γ-GT) activity,[10] and depigmentation of these cells.[11,12] Such observations have led to the hypothesis[13] that an early step in the pathogenesis of PD is an elevated γ-GT-mediated translocation of cysteine (CySH) or GSH[14,15] into pigmented SN cell bodies that normally contain little or none of these sulfhydryl compounds.[16,17] *In vitro* studies[13,17] suggest that increased cytoplasmic CySH levels would divert the neuromelanin pathway by scavenging DA-*o*-quinone to give soluble cysteinyl conjugates of DA with concomitant progressive depigmentation of SN cells and an increased 5-*S*-CyS-DA/DA ratio. Subsequent autoxidation of cysteinyldopamines has further been proposed to lead to products that might include endotoxins that contribute to nigral cell death and PD.[13]

The neurodegeneration that occurs in PD also affects noradrenergic neurons that project from their pigmented cell bodies in the locus ceruleus (LC).[18,19] These cell bodies are pigmented because of autoxidation of norepinephrine (**1**) to an *o*-quinone that polymerizes to neuromelanin.[3,20] Little is known about the changes that occur in the LC in PD. However, LC and SN neurons are similar in that they both contain relatively high cytoplasmic levels of the catecholamine neurotransmitters **1** and DA, respectively, that are easily oxidized to *o*-quinone intermediates and thence to neuromelanin, and both depigment and degenerate in PD. Taken together, such observations might indicate that similar mechanisms underlie the pathological processes that occur in both SN and LC cell bodies in PD. Interestingly, noradrenergic neurons that project from the LC to the cortex and hippocampus also degenerate in Alzheimer's Disease (AD)[21] and following a transient ischemic insult.[22] However, unlike PD, in which the neuropathological processes occur in SN and LC cell bodies,[2,23] the neurodegenerative processes that occur in AD and following transient cerebral ischemia are believed to occur in terminal regions of noradrenergic and other neurons.[24−26] Furthermore, nerve terminals differ from cell bodies in that they contain significant concentrations of GSH and, presumably to a lesser extent, its biosynthetic precursor CySH.[16] Many lines of evidence indicate that terminal regions of the brain vulnerable to degeneration in AD and transient cerebral ischemia, such as the cortex, are subject to oxidative stress, *i.e.*, damage deriving from abnormally high levels of oxygen radical species.[27−33] Ischemia/reperfusion also results in significant depletion of GSH in the cortex without a corresponding increase in GSSG.[34,35]

Oxygen radical-mediated and other oxidative damage in brain tissue is widely believed to primarily affect membrane lipids, proteins, and nucleic acids.[36] However, noradrenergic terminals that degenerate in AD and following an ischemic insult employ a neurotransmitter, **1**, that is a very easily oxidized compound. It is not inconceivable, therefore, that in these brain disorders **1** is oxidized within noradrenergic terminals to an

* Corresponding author.
[⊗] Abstract published in *Advance ACS Abstracts,* April 15, 1996.

S0022-2623(96)00016-7 CCC: $12.00

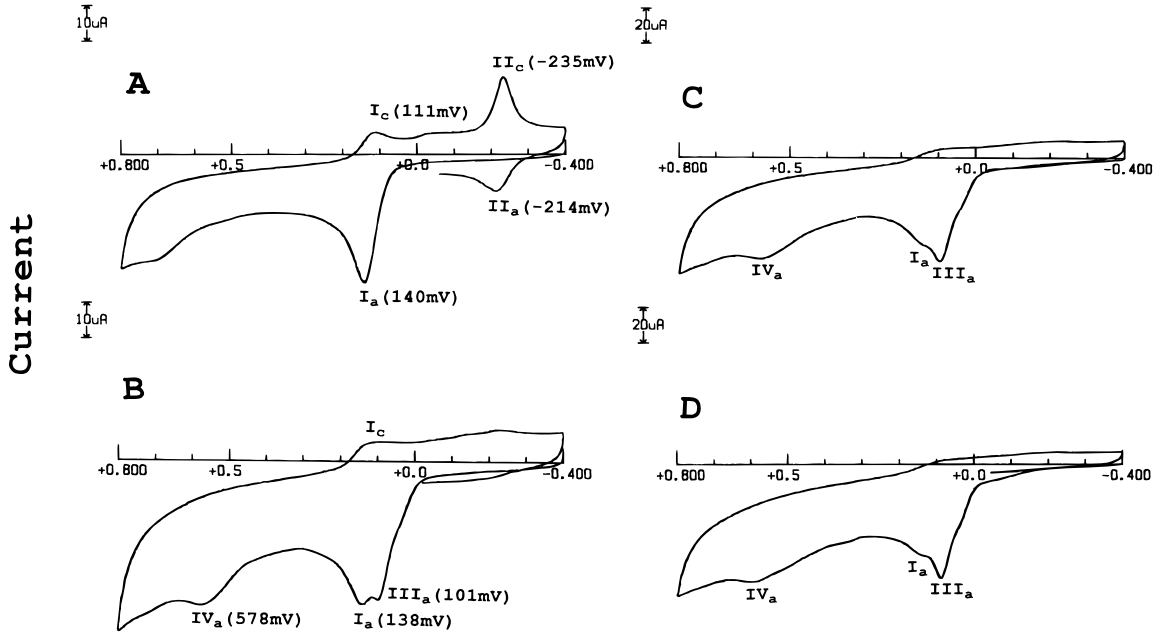

Figure 1. Cyclic voltammograms at the PGE of 0.5 mM norepinephrine (**1**) in pH 7.4 phosphate buffer ($\mu = 1.0$) in the presence of (A) 0 mM CySH, (B) 0.25 mM CySH, (C) 0.5 mM CySH, and (D) 1.0 mM CySH. Sweep rate: 50 mV s^{-1}. All voltammograms were initiated at −400 mV.

o-quinone that is scavenged by CySH and that the resulting cysteinyl conjugates of the neurotransmitter are further oxidized to endotoxins that might contribute to the degeneration of these neurons. In essence, it is hypothesized that the vulnerability of pigmented noradrenergic LC cell bodies, which normally contain little or no GSH or CySH, to degeneration in PD is linked to the fact that **1** is autoxidized in these neurons. The pathological processes in PD are hypothesized to be triggered by an aberrant increase in cytoplasmic levels of CySH or GSH that divert the neuromelanin pathway to give endotoxic metabolites. By contrast, the vulnerability of certain noradrenergic nerve terminals to degeneration in AD or following an ischemic insult might be related to aberrant oxidation of **1** to an *o*-quinone that reacts with endogenous CySH or GSH to give the same or similar endotoxins. It was clearly of interest, therefore, to explore the influence of CySH on the oxidation chemistry of **1** at physiological pH. A number of reasons led us to employ electrochemical techniques in this initial study. Thus, controlled potential electrolysis provides a way of maintaining very precise control of oxidizing conditions. Furthermore, cyclic voltammetry often permits considerable insights into reaction intermediates and mechanisms and provides an extremely convenient method to measure redox potentials of both intermediates and products. Because of the fact that the chemical[3] (*e.g.*, autoxidation) and electrochemical[20] oxidations of **1** (and related catecholamines) both generate an *o*-quinone intermediate as the proximate reaction product, it was anticipated that the results of this investigation might ultimately provide valuable insights into more biologically relevant oxidations of this neurotransmitter in the presence of CySH mediated by molecular oxygen or oxygen radical species. The principal goals of this investigation were to elucidate the influence of CySH on the oxidation chemistry of **1** with particular emphasis on mechanistic pathways and characterizations of major reaction intermediates and products. Furthermore, reaction products were screened for neurobiological activity following administration into the brains of mice.

Scheme 1

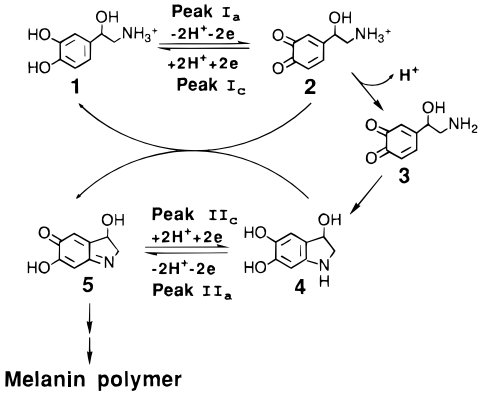

Results

Cyclic Voltammetry. A cyclic voltammogram of **1** (0.5 mM) at a pyrolytic graphite electrode (PGE) in pH 7.4 phosphate buffer at a sweep rate (ν) of 50 mV s^{-1} is presented in Figure 1A. On the initial anodic sweep, peak I_a appears at a peak potential (E_p) of 140 mV and corresponds to the oxidation (2*e*, $2H^+$) of **1** to *o*-quinone **2** (Scheme 1).[20,37] An indistinct second peak also appears at *ca.* 700 mV (Figure 1A) that might correspond to oxidation of the side chain residue of *o*-quinone **2**.[38] Following scan reversal, peak I_c ($E_p = 111$ mV) corresponds to the reversible reduction of *o*-quinone **2** to **1**. Previous investigators[20,37] have established that at pH 7.4 deprotonation of **2** yields **3** which cyclizes to 3,5,6-trihydroxyindoline (**4**) that is further oxidized (2*e*, $2H^+$) by **2** at the electrode surface to give the aminochrome **5** and **1**. Aminochrome **5** is the species responsible for

peak II_c ($E_p = -235$ mV) observed in cyclic voltammograms of **1** and corresponds to its reduction ($2e$, $2H^+$) to **4**. Peak II_a ($E_p = -214$ mV), observed on the second anodic sweep, corresponds to the reversible oxidation of **4**, formed in the peak II_c reduction, to **5**. At slow sweep rates ($v \leq 50$ mV s^{-1}) the peak current (i_p) for reduction peak I_c is small compared to that for oxidation peak I_a owing to the relatively rapid reaction between **2** and **4** (Scheme 1). However, with increasing sweep rates i_p for peak I_c grows relative to that for peak I_a until the two peaks become of equal size ($v > 10$ V s^{-1}). Correspondingly, the peak II_c/peak II_a couple decreases and at $v > 10$ V s^{-1} disappears.

Cyclic voltammograms ($v = 50$ mV s^{-1}) of **1** (0.5 mM) in the presence of CySH (0.25−1.0 mM) at pH 7.4 are presented in Figure 1B−D. The presence of CySH clearly results in some significant alterations in the cyclic voltammetric behaviors of **1**. Thus, with increasing concentrations of CySH, reduction peak I_c and the peak II_c/peak II_a couple decrease and at a concentration of ≥0.5 mM disappear (Figure 1C,D). Furthermore, at the lowest CySH concentration studied (0.25 mM; CySH/**1** mole ratio = 0.5) two new major oxidation peaks appear. Peak III_a ($E_p = 101$ mV; $v = 50$ mV s^{-1}) appears at more negative potentials than peak I_a of **1** ($E_p = 138$ mV) and peak IV_a ($E_p = 578$ mV) at more positive potentials (Figure 1B). With increasing CySH concentrations, peak III_a becomes the predominant peak (Figure 1C,D) and shifts toward slightly more negative potentials. Thus, E_p values ($v = 50$ mV s^{-1}) for peak III_a measured with 0.5, 1.0, and 2.5 mM CySH were 96, 90, and 86 mV, respectively. Optimal resolution between peaks III_a and I_a was obtained with 0.5 mM **1** and 0.25 mM CySH using a slow sweep rate (10 mV s^{-1}). Under these conditions, E_p for peak III_a was 76 mV and E_p for peak I_a was 136 mV (*i.e.*, $\Delta E_p = 60$ mV). With increasing sweep rate, E_p for peak III_a shifts toward more positive potentials and at $v \geq 500$ mV s^{-1} peaks III_a and I_a merge to give a single peak. Taken together, the above results suggest that there is a rapid reaction between the proximate oxidation product of **1**, *o*-quinone **2**, and CySH. This reaction not only scavenges **2**, as demonstrated by the decrease and disappearance of reduction peak I_c with increasing CySH concentrations (Figure 1B−D) but also blocks formation of **4** and **5** as shown by the elimination of the peak II_c/peak II_a couple. Over the potential ranges employed in cyclic voltammetric experiments, CySH exhibits no oxidation or reduction peaks at the PGE. Accordingly, the reaction between **2** and CySH must also yield the product(s) responsible for oxidation peak III_a and subsequent oxidation of this (these) compound(s) must yield the species responsible for oxidation peak IV_a.

Controlled Potential Electro-Oxidation Studies. At $v = 10$ mV s^{-1} the E_p values for oxidation peak III_a observed in voltammograms of 0.5 mM **1** in the presence of 0.25, 0.5, 1.0, and 2.5 mM CySH at pH 7.4 were 76, 74, 72, and 70 mV, respectively. Accordingly, controlled potential electro-oxidations of **1** in the presence of free CySH at pH 7.4 were carried out at 70 mV. Because the major goal of this investigation was to identify the initial steps in the oxidation chemistry of the **1**/CySH system, all controlled potential electrolyses were terminated after ≤30 min in order to minimize secondary oxidation reactions.

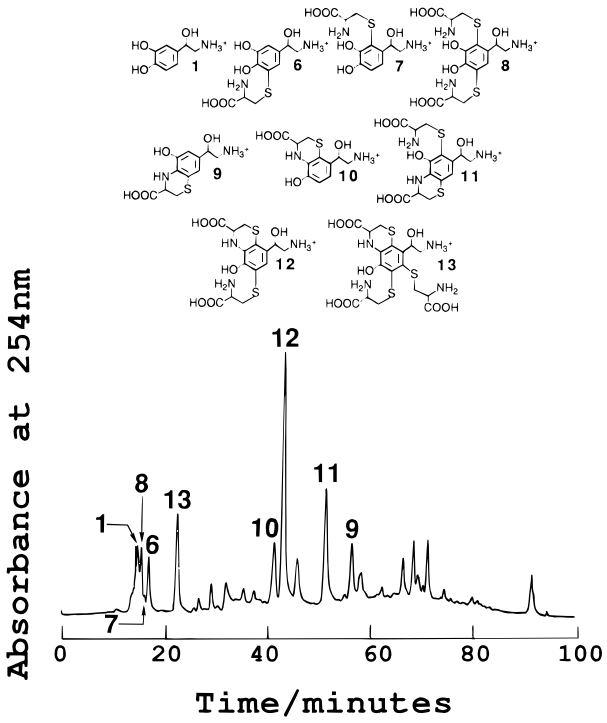

Figure 2. HPLC chromatogram (method I) of the product solution formed following controlled potential electro-oxidation of 0.5 mM norepinephrine (**1**) in the presence of 1.0 mM CySH in pH 7.4 phosphate buffer for 30 min at 70 mV.

In the absence of free CySH, controlled potential electrolyses of **1** (0.5 mM) at 70 mV and pH 7.4 were very slow. After 30 min the solution had a pale orange color. HPLC analysis (method I) of this product solution revealed that less than 10% of **1** had been oxidized, and a single significant product was formed having a retention time (t_R) of 28.5 min. In the HPLC mobile phase (pH 2.15) this orange product exhibited a UV−visible spectrum with $\lambda_{max} = 488$, 290, and 216 nm and a thermospray mass spectrum with an intense pseudomolecular ion (MH^+) at $m/e = 166$ (40%) expected for aminochrome **5**. Controlled potential electro-oxidation of **1** (0.5 mM) in the presence of CySH (0.5−1.0 mM) at pH 7.4 and 70 mV caused the initially colorless solution to become a very pale yellow color. HPLC analysis (method I) of the solution formed after 30 min revealed that a complex mixture of products was formed (Figure 2). Using preparative HPLC (method II) to isolate individual compounds, and an independent electrochemical synthesis, eight of the major products were isolated and spectroscopically identified (see the Experimental Section). The structures of these products are presented in Figure 2 and include 5-*S*-cysteinylnorepinephrine (**6**), 2-*S*-cysteinylnorepinephrine (**7**), and 2,5-bi-*S*-cysteinylnorepinephrine (**8**) in addition to dihydrobenzothiazines **9**−**13**. When electrolyses were permitted to proceed for periods greater than 30 min, the chromatographic peaks for **6**−**13** systematically decreased, and correspondingly, several peaks at $t_R >$ 65 min increased in height. These observations indicate that the compounds responsible for the latter chromatographic peaks are secondary products and, hence, will not be discussed further.

Cyclic Voltammetry of Cysteinyl Conjugates 6−8 and Dihydrobenzothiazines 9−13. Cyclic voltammograms ($v = 50$ mV s^{-1}) of **6**−**13** in pH 7.4

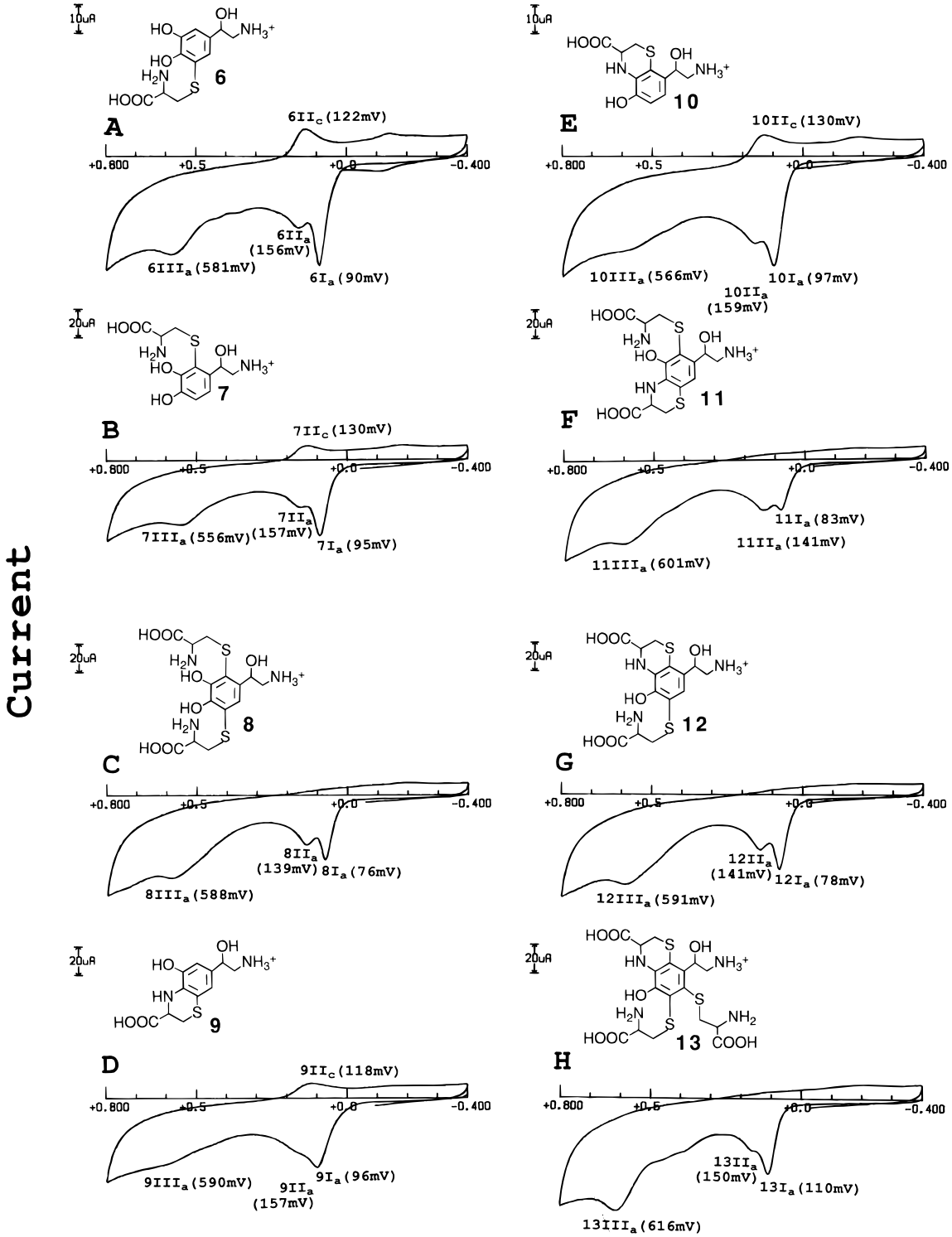

Figure 3. Cyclic voltammograms at the PGE of 0.5 mM solutions of **6**−**13**, in pH 7.4 phosphate buffer. Sweep rate: 50 mV s^{-1}.

phosphate buffer (Figure 3) reveal that each of these compounds exhibit three major oxidation peaks (I_a, II_a, and III_a) on the initial anodic sweep. After scan reversal, compounds **6**, **7**, **9**, and **10** exhibited reduction peaks that were reversibly coupled to oxidation peak II_a. A summary of E_p values for peaks I_a, II_a, II_c, and III_a for compounds **6**−**13** at pH 7.4 at sweep rates of 10 and 50 mV s^{-1} is presented in Table 1. These results reveal that the E_p values for the primary oxidation peak I_a of cysteinyl conjugates **6**−**8** and dihydrobenzothiazines **9**−**13** all occur at more negative potentials than that for peak I_a of **1**, indicating that these products are appreciably more easily oxidized than the latter neurotransmitter. With increasing sweep rate, peak III_a observed in cyclic voltammograms of **1** (0.5 mM) in the presence of free CySH (0.25−2.5 mM) shifts toward more positive potentials whereas peak I_a (corresponding to oxidation of **1**) remains virtually constant (Table 1). Similarly, peaks **6**I_a−**13**I_a also shift to more positive potentials with increasing ν.

Table 1. Peak Potentials (E_p) for Oxidation and Reduction Peaks Observed in Cyclic Voltammograms of **1**, **1** + CySH, and Compounds **6**−**13** at pH 7.4[a]

Compound[b]	Peak	Ep for peak/mV *vs.* SCE at ν = 10 mVs^{-1}	at ν = 50 mVs^{-1}
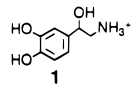 **1**	I_a	136	140
1 + 0.25 mM CySH	III_a	76	101
	I_a	136	138
1 + 0.5 mM CySH	III_a	74	96
	I_a	136	138
1 + 1.0 mM CySH	III_a	72	90
	I_a	136	138
1 + 2.0 mM CysH	III_a	70	86
	I_a	136	138
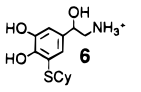 **6**	**6**I_a	66	90
	6II_a	162	156
	6II_c	122	122
	6III_a		581
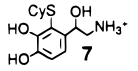 **7**	**7**I_a	72	95
	7II_a	159	157
	7II_c	132	130
	7III_a		556
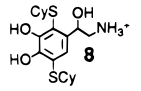 **8**	**8**I_a	53	76
	8II_a	123	139
	8II_c		
	8III_a	586	588
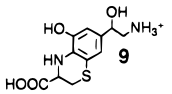 **9**	**9**I_a	84	96
	9II_a	160	157
	9II_c	120	118
	9III_a		590
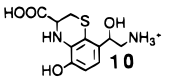 **10**	**10**I_a	84	97
	10II_a	162	159
	10II_c	130	130
	10III_a		566
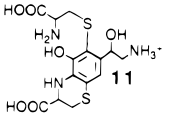 **11**	**11**I_a	64	83
	11II_a	123	141
	11II_c		
	11III_a	599	601
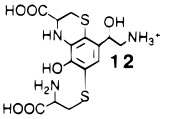 **12**	**12**I_a	58	78
	12II_a	123	141
	12II_c		
	12III_a	588	591
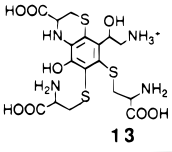 **13**	**13**I_a	88	110
	13II_a	129	150
	13II_c		
	13III_a	613	616

[a] Voltammograms recorded at the PGE in pH 7.4 phosphate buffer (μ = 1.0).
[b] Concentrations of all compounds, except CySH, were 0.5 mM.

Oxidations of Cysteinyl Conjugates 6−8. Figure 4 A presents a chromatogram (HPLC method I) of the product solution formed following controlled potential electro-oxidation of **6** (0.5 mM) at 70 mV for 25 min in pH 7.4 buffer and clearly indicates that the major initial product is dihydrobenzothiazine **9**. Similarly, controlled potential electro-oxidation of **7** (0.5 mM) at 70 mV for 25 min yields dihydrobenzothiazine **10** as the major initial product (Figure 4B). Oxidation of the 2,5-bi-*S*-cysteinyl conjugate **8** under similar conditions yields dihydrobenzothiazine **12** as the major product and dihydrobenzothiazine **11** as a minor product (Figure 4C). These results indicate that cysteinyl conjugates **6** and **7** are precursors of dihydrobenzothiazines **9** and **10**, respectively, and that the bi-*S*-cysteinyl conjugate **8** is the precursor of dihydrobenzothiazines **11** and, particularly, **12**. When the oxidation reactions of **6**−**8** were continued for longer periods of time, the chromatographic peaks corresponding to their various dihydrobenzothiazine products systematically decreased and disappeared and the relatively minor peaks having t_R values ≥ 60 min in Figure 4A−C correspondingly grew larger and the solution developed a bright yellow color. These yellow secondary oxidation products, however, remain to be identified.

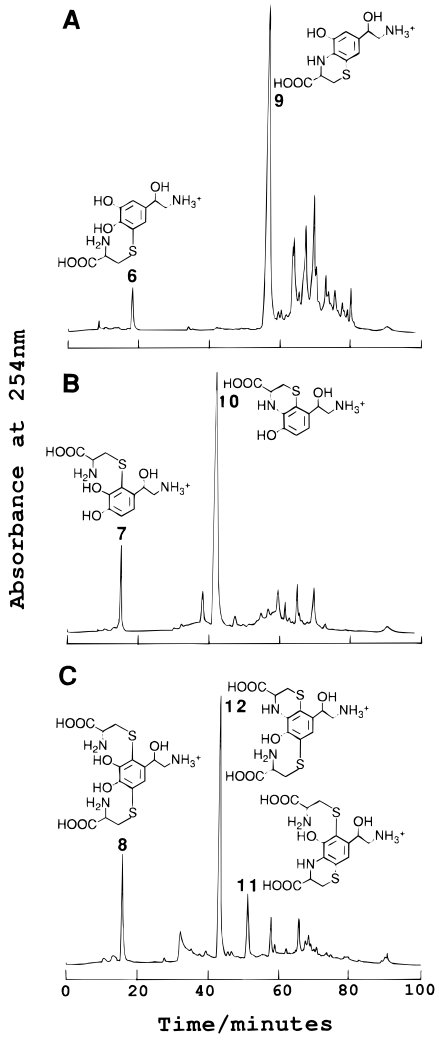

Figure 4. HPLC chromatograms (method I) of the product solutions formed following controlled potential electro-oxidation of 0.5 mM solutions of (A) **6**, (B) **7**, and (C) **8** in pH 7.4 phosphate buffer at 70 mV for 25 min.

Controlled potential electro-oxidation of dihydrobenzothiazine **9** in the presence of excess free CySH at 70 mV and pH 7.4 initially gave its 6-*S*-cysteinyl conjugate **11** as the major product (Figure 5A). Oxidation of dihydrobenzothiazine **10** in the presence of free CySH under identical conditions gave its 6-*S*-cysteinyl conjugate **12** as the major initial product along with smaller yields of its 6,7-bi-*S*-cysteinyl conjugate **13** (Figure 5B). Oxidation of **12** in the presence of free CySH under the same conditions gave **13** as the major initial product (data not shown). More prolonged electro-oxidations of **9**, **10**, and **12** in the presence of CySH resulted in the formation of a bright yellow solution containing many secondary products (which appear as minor products in Figure 5A,B) that remain to be identified.

Reaction Pathways

The results of cyclic voltammetry experiments indicate that CySH scavenges *o*-quinone **2**, the proximate oxidation product of **1** (Figure 1A−C). A key observation in cyclic voltammograms of **1** in the presence of free CySH is the appearance of oxidation peak III_a at less positive potentials than peak I_a of **1**. The i_p for peak III_a compared to that for peak I_a in cyclic voltammograms of **1** even in the presence of relatively small amounts of CySH (Figure 1B) reveals that the reaction between **2** and CySH is extensive at potentials corresponding to the foot of peak I_a to form a product(s) that is more easily oxidized than **1**. E_p for peak III_a (70−76 mV, $\nu = 10$ mV s^{-1}, pH 7.4) observed in cyclic voltammograms of **1** (0.5 mM) in the presence of free CySH (0.25−2.5 mM) is very close to the primary oxidation peaks of cysteinyl conjugates **6** (E_p for peak **6**I_a = 66 mV) and **7** (E_p for peak **7**I_a = 72 mV). Since **6** and **7** must logically be the initial products formed between **2** and CySH it is reasonable to conclude that peak III_a corresponds in part to oxidation of **6** and **7**. At potentials corresponding to the foot of peak I_a of **1**, CySH must rapidly scavenge **2** to give cysteinyl conjugates **6** and **7**, thus momentarily depleting the surface concentration of this *o*-quinone. Nernstian considerations, therefore, demand that additional **1** is oxidized to **2** at these low potentials with the result that CySH facilitates oxidation of the neurotransmitter. The fact that **6** and **7** are also more easily oxidized than **1** accounts for further enhancement of the current observed at peak III_a.

Controlled potential electrolysis of **1** in the presence of free CySH at potentials corresponding to peak III_a results in the rapid oxidation of the neurotransmitter compared to its rate of oxidation in the absence of CySH. However, only rather low yields of **6**, **7**, and **8** are formed (Figure 2) because of the ease of further oxidation of these cysteinyl conjugates of **1** (Table 1). The major initial products of this electrochemically driven oxidation reaction include dihydrobenzothiazines **9** and **10** and their cysteinyl conjugates **11** and **12** + **13**, respectively (Figure 2). This result was somewhat surprising because (1) intramolecular cyclization of *o*-quinones formed upon oxidation of **6** and **7** would be expected to yield *o*-quinone imines not their corresponding reduced forms, *i.e.*, dihydrobenzothiazines **9** and **10**, respectively; (2) dihydrobenzothiazines **9** and **10** (and **11**−**13**) are also very easily oxidized compounds (Table 1) and would therefore be expected to be further oxidized at controlled potentials corresponding to peak III_a (70 mV). In an earlier investigation[13] it was proposed that structurally related *o*-quinone imines were maintained in their reduced (dihydrobenzothiazine) state by CySH. However, in this investigation it has been demonstrated that even in the absence of free CySH cysteinyl conjugates **6** and **7** are initially oxidized to dihydrobenzothiazines **9** and **10**, respectively (Figure 4) at peak III_a potentials (along with several minor unidentified products). These observations imply that upon cyclization of the *o*-quinones formed by oxidation of **6** and **7** a chemical pathway must exist whereby the resulting bicyclic *o*-quinone imines are reduced to the corresponding dihydrobenzothiazines. Insights into such a pathway can be derived from the cyclic voltammetric behaviors of cysteinyl conjugates such as **6** and **7** and dihydrobenzothiazines **9** and **10** at pH 7.4. To illustrate, Figure

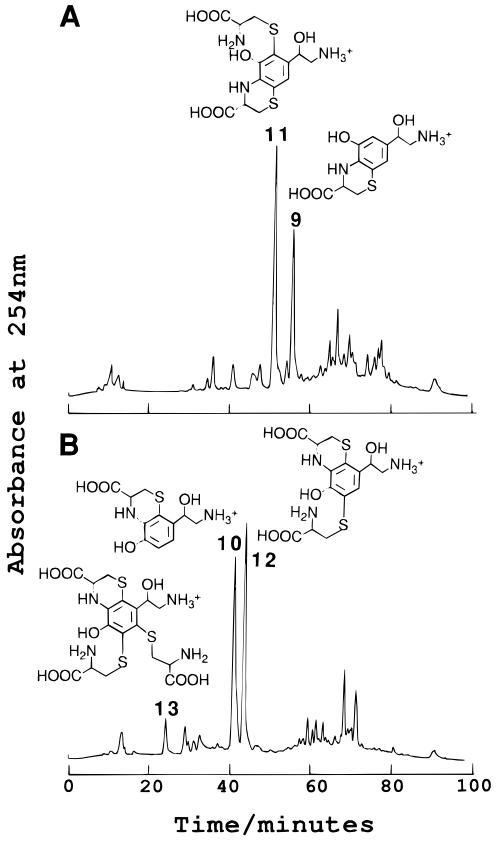

Figure 5. HPLC chromatograms (method I) of the product solutions obtained following controlled potential electro-oxidation of 0.1 mM solutions of dihydrobenzothiazines (A) **9** and (B) **10** in pH 7.4 phosphate buffer in the presence of 0.5 mM CySH for 25 min at 70 mV.

6A presents a slow sweep rate ($\nu = 10$ mV s^{-1}) cyclic voltammogram of dihydrobenzothiazine **10**. On the initial anodic sweep two well-defined oxidation peaks **10**I_a (E_p = 84 mV) and **10**II_a (E_p = 162 mV) appear. Following scan reversal reduction peak **10**II_c (E_p = 130 mV) forms a reversible couple with oxidation peak **10**II_a. With increasing sweep rates, however, the i_p values for the peak **10**II_a/peak **10**II_c couple decrease (Figure 6B), and at $\nu \geq 5$ V s^{-1} this couple disappears (Figure 6C). Under the latter conditions a new reduction peak **10**I_c (E_p = 102 mV; $\nu = 5$ V s^{-1}) appears that forms a reversible couple with peak **10**I_a (Figure 6C). Such observations suggest that at slow sweep rates the proximate product of the peak **10**I_a reaction undergoes a chemical reaction to give the species responsible for the peak **10**II_a/peak **10**II_c couple. However, at fast sweep rates there is insufficient time for this chemical reaction to occur with the result that the peak **10**II_a/peak **10**II_c couple does not appear and peak **10**I_c corresponds to the reduction of the proximate product formed at peak **10**I_a. These observations are rationalized by proposing that dihydrobenzothiazines **10** undergoes a one-electron oxidation in the peak **10**I_a reaction to give radical cation **14** (Scheme 2). At fast sweep rates, therefore, peak **10**I_c corresponds to the reversible one-electron reduction of **14** to **10**. However, at slower sweep rates deprotonation of **14** yields the neutral radical **15** that is further oxidized (1*e*) to *o*-quinone imine **16** in the peak **10**II_a reaction. After scan reversal, peak **10**II_c therefore corresponds to the reversible reduction of **16** to **15**.

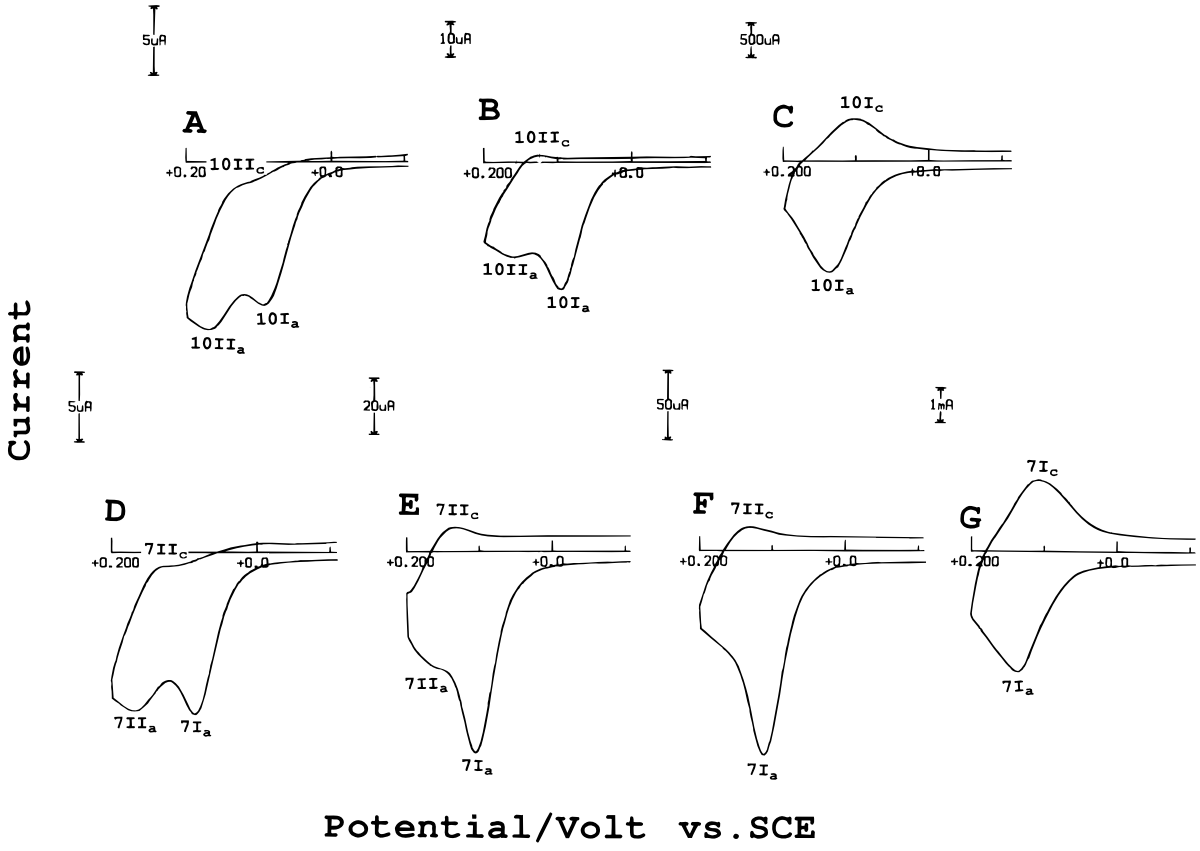

Figure 6. Cyclic voltammograms at the PGE of a 0.5 mM solution of dihydrobenzothiazine **10** in pH 7.4 phosphate buffer at a sweep rate of (A) 10 mV s^{-1}, (B) 50 mV s^{-1}, and (C) 5.0 V s^{-1} and of 0.5 mM 2-*S*-cysteinylnorepinephrine (**7**) at a sweep rate of (D) 10 mV s^{-1}, (E) 100 mV s^{-1}, (F) 200 mV s^{-1}, and (G) 10 V s^{-1}.

Scheme 2

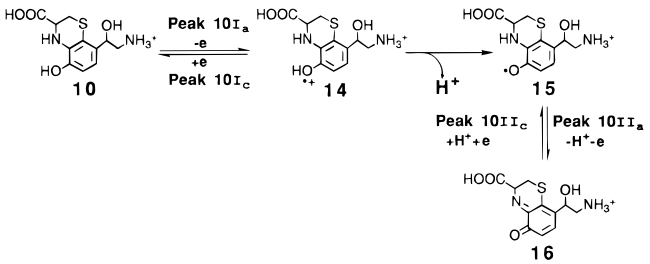

Scheme 3

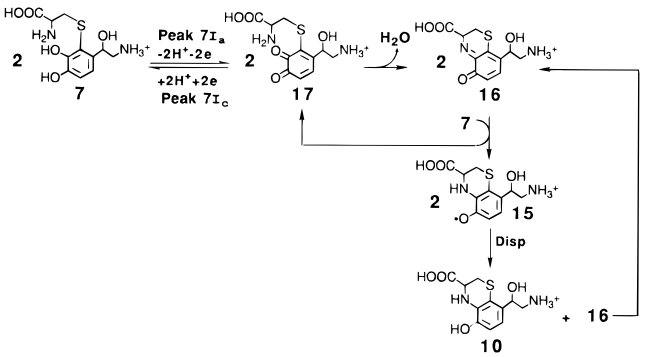

A slow sweep rate ($\nu = 10$ mV s^{-1}) cyclic voltammogram of cysteinyl conjugate **7** at pH 7.4 is presented in Figure 6D. On the initial anodic sweep oxidation peak **7**I$_a$ ($E_p = 72$ mV) and peak **7**II$_a$ ($E_p = 159$ mV) appear. After scan reversal, reduction peak **7**II$_c$ ($E_p = 132$ mV) forms a reversible couple with oxidation peak **7**II$_a$. The E_p values for oxidation peaks **7**II$_a$ and **10**II$_a$ and for peaks **7**II$_c$ and **10**II$_c$ are virtually identical. With increasing sweep rate, i_p for oxidation peak **7**II$_a$ decreases relative to that for oxidation peak **7**I$_a$ (Figure 6E) and ultimately disappears (Figure 6F). A parallel decrease in i_p for reduction peak **7**II$_c$ does not occur. However, at $\nu \geq 5$ V s^{-1} peak **7**II$_c$ disappears and a new reduction peak **7**I$_c$ appears and forms a reversible couple with oxidation peak **7**I$_a$ (Figure 6G). Under the latter conditions, peak **7**I$_a$ corresponds to the oxidation (2*e*, 2H$^+$) of cysteinyl conjugate **7** to *o*-quinone **17** and peak **7**I$_c$ to the reverse reaction (Scheme 3). At slower sweep rates, however, there is sufficient time for intramolecular cyclization of **17** to *o*-quinone imine **16**. Thus, oxidation of **7** leads directly to *o*-quinone imine **16**, the species responsible for reduction peak **10**II$_c$ in cyclic voltammograms of cysteinyl conjugate **7** (Figure 6D–F). The E_p for peak **7**II$_c$ is clearly at more positive values than that for oxidation peak **7**I$_a$. Thus, *o*-quinone imine **16** must be capable of chemically oxidizing cysteinyl conjugate **7** in a reaction that generates *o*-quinone **17** and radical **15** as conceptualized in Scheme 3. This conclusion is supported by the observation that at slow sweep rates cyclic voltammograms of **7** exhibit peak **7**II$_a$ (equivalent to peak **10**II$_a$ in cyclic voltammograms of **10**) corresponding to oxidation of radical **15**, formed in this chemical reaction, to *o*-quinone imine **16** (Figure 6D). At faster sweep rates, however, reaction between **16** and **7** to generate radical **15** is less extensive, and hence i_p for oxidation peak **7**II$_a$ decreases whereas peak **7**IIc (corresponding to reduction of **16**) remains a significant feature of cyclic voltammograms of **7** (Figure 6E,F). The major initial product of controlled potential electro-oxidation of **7** at peak III$_a$ potentials is dihydrobenzothiazine **10** (Figure 4B). In

Scheme 4

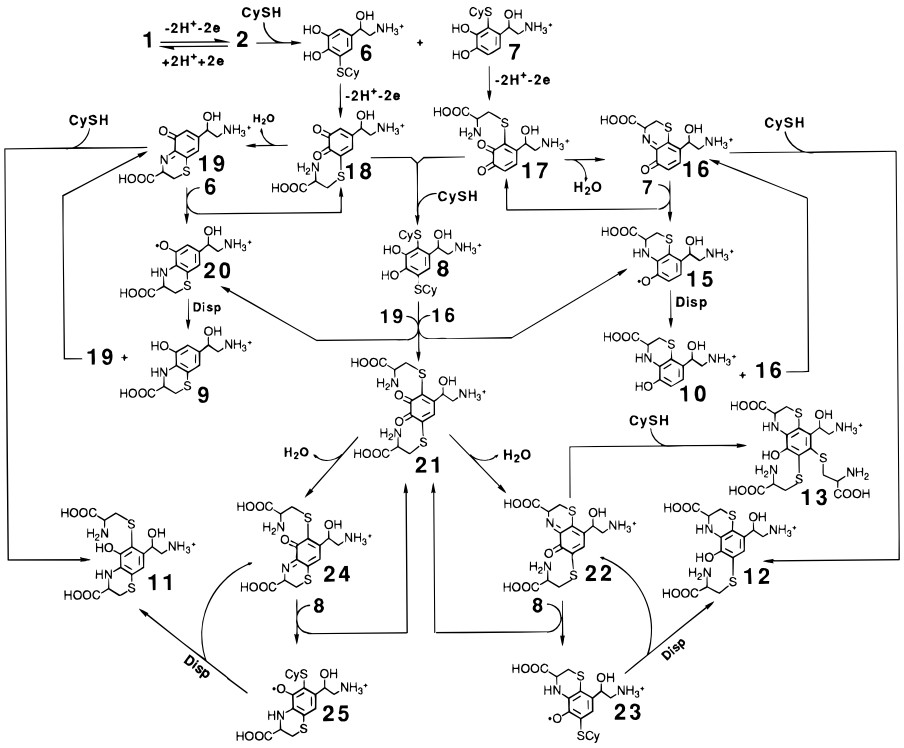

view of this observation, radical **15** must disproportionate to give **10** and **16**. The pathway conceptualized in Scheme 3 predicts that once oxidation of cysteinyl conjugate **7** is initiated the reaction should become self-sustaining (autocatalytic). Experimentally, however, this is not the case indicating that *o*-quinone imine **16** probably undergoes additional reactions that lead to several other as yet unidentified products (Figure 4B). The cyclic voltammetric behaviors of cysteinyl conjugate **6** and dihydrobenzothiazine **9** are very similar to those described for **7** and **10**, respectively. Furthermore, controlled potential electro-oxidation of **6** at peak III_a potentials gives **9** as the major initial product (Figure 4A). Accordingly, it was concluded that the oxidation chemistry of **6** and **9** is similar to that proposed for **7** (Scheme 3) and **10** (Scheme 2), respectively.

On the basis of the foregoing discussion, the reaction sequences presented in Scheme 4 are proposed to account for the major initial products of the controlled potential electro-oxidation of **1** at pH 7.4 in the presence of CySH at peak III_a potentials. Thus, as noted previously, oxidation of **1** (2*e*, $2H^+$) leads to *o*-quinone **2**. Nucleophilic addition of CySH to **2** then forms cysteinyl conjugates **6** and **7**. Addition of CySH (2.0−4.0 mM) to *o*-quinone **2** (*ca*. 1.0 mM), synthesized by controlled potential electro-oxidation of **1** at 1.0 V in 0.1M HCl, results in formation of conjugates **6** and **7** in relative yields of approximately 3:1 (see the Experimental Section). Similar studies could not be carried out at pH 7.4 because of the instability of **2**. Nevertheless, chromatograms of product solutions formed following oxidation of **1** in the presence of CySH always indicated that yields of **6** were significantly greater than **7** (Figure 2). Such observations suggest that at pH 7.4 nucleophilic addition of CySH to **2** occurs predominantly, but not exclusively, at the C(5)-position. Further oxidation (2*e*, $2H^+$) of **6** and **7** leads to *o*-quinones **18** and **17**, respectively, that can each react by at least three pathways. The first of these pathways results from intramolecular cyclizations of **17** and **18** to **16** and **19**, respectively (Scheme 4). The latter quinone imines then diffuse away from the electrode and chemically oxidize cysteinyl conjugates **6** and **7** and hence provide routes to dihydrobenzothiazines **9** and **10** as conceptualized in Scheme 4 and discussed in detail in connection with Schemes 2 and 3.

A second pathway involves nucleophilic addition of CySH to *o*-quinone imines **19** and **16** to give the cysteinyl dihydrobenzothiazine conjugates **11** and **12**, respectively (Scheme 4). These pathways are experimentally supported by the observation that controlled potential electro-oxidation of dihydrobenzothiazines **9** and **10** in the presence of free CySH at peak III_a potentials yield cysteinyl conjugates **11** (Figure 5A) and **12** (Figure 5B), respectively, as the major initial products. However, in these reactions formation of *o*-quinone imines **16** and **19** results from a multistep pathway. To illustrate, at peak III_a potentials, dihydrobenzothiazine **10**, for example, is initially oxidized to radical cation **14** (Scheme 2). Following deprotonation, radical **15** then disproportionates to *o*-quinone imine **16** and **10** (Scheme 3).

The third reaction pathway deriving from *o*-quinones **17** and **18** involves nucleophilic addition of CySH to give the 2,5-bi-*S*-cysteinyl conjugates of **1**, *i.e.*, **8** (Scheme 4; Figure 2). Controlled potential electro-oxidation of **8** at peak III_a potentials even in the absence of free CySH yields the cysteinyl dihydrobenzothiazines **11** (minor product) and **12** (major product) (Figure 4C). Accordingly, by analogy with reaction pathways discussed previously, it can be concluded that **8**, a very easily oxidized compound (Table 1), is chemically oxidized by **16**/**19** to *o*-quinone **21** that undergoes intramolecular cyclization to *o*-quinone imines **22** (major route) and **24** (minor route). Subsequent oxidation of **8** by **22** and **24** then leads to radicals **23** and **25**, respectively. Dispro-

portionations of **23** and **25** then yield dihydrobenzothiazines **12** (and **22**) and **11** (and **24**), respectively.

In view of the fact that dihydrobenzothiazine **12** is the major initial product of oxidation of **1** in the presence of CySH (Figure 2) under the conditions employed in this investigation, *o*-quinone imine **22** must represent a major intermediate species. This no doubt accounts for the appearance of **13**, formed by nucleophilic addition of CySH to **22** (Scheme 4). This conclusion is further confirmed by the fact that oxidation of **12** in the presence of free CySH yields **13**.

Biological Studies

Preliminary *in vivo* experiments were carried out to assess the toxicity and behavioral responses evoked when **6**−**13** were administered into the brains of laboratory mice. In these experiments, each compound was dissolved in 5 μL of isotonic saline and injected into the vicinity of the left lateral ventricle while animals were under a light ether anesthesia. The LD_{50} value, used as a measure of toxicity and defined as the dose of injected compound (expressed as free base) at which 50% of the treated animals died within 1 h, was determined using the statistical method of Dixon.[39]

Dihydrobenzothiazines **9** and **10** were lethal, having experimental LD_{50} values of 17.8 ± 1.3 μg (mean ± standard deviation) and 23.4 ± 1.3 μg, respectively. Doses of **9** ranging from 5 to 100 μg and of **10** ranging from 10 to 100 μg were employed to determine these LD_{50} values. The behavioral responses evoked by **9** and **10** were very similar. The responses described below refer to those evoked at the LD_{50} dose. Following recovery from the ether anesthetic, animals initially either circled contralateral to the site of injection or moved slowly in a backward direction for *ca*. 2−10 min. Subsequently, experimental animals exhibited episodes of rapid running, jumping, rolling repetitively along the head−tail axis, and squeaking. Episodes of severe shivering were also observed. Animals treated with **11** (60−100 μg) and **7** (100 μg) initially circled contralateral to the site of injection followed by episodes of rapid running. At the 100 μg dose level **6**, **8**, **12**, and **13** evoked no obvious behavioral response and all animals survived. Control animals treated with 5 μL of isotonic saline exhibited none of the above behavioral effects noted with **7**, **9**, **10**, and **11** and all survived.

Discussion

The results of this investigation reveal that CySH can divert the oxidation pathway of **1** to black melanin polymer (Scheme 1) by scavenging *o*-quinone **2** to form **6** and **7** (Scheme 4). However, these cysteinyl conjugates of **1** are appreciably more easily oxidized than the neurotransmitter (Table 1, Figure 3A,B) to give *o*-quinones **17** and **18** that are the precursors of dihydrobenzothiazines **9**−**13** (Scheme 4). The key step in the pathways leading to these dihydrobenzothiazines is the intramolecular cyclization of *o*-quinones **17**, **18**, and **21** to give bicyclic *o*-quinone imines **16**, **19**, and **22**/**24**, respectively. It is conceivable that these *o*-quinone imines might be reduced to the corresponding dihydrobenzothiazines by CySH.[13] However, the present results demonstrate that, even in the absence of free CySH, oxidation of cysteinyl conjugates **6**, **7**, and **8** leads to dihydrobenzothiazines **9**, **10**, and **11**/**12**, respectively, as major initial products. This unusual observation can be traced to the fact that *o*-quinone imines **19**, **16**, and **22/24** are capable of oxidizing cysteinyl conjugates **6**, **7**, and **8**, respectively, and are therefore reduced to the corresponding dihydrobenzothiazines. Indeed, the formation of such dihydrobenzothiazines provides evidence to support the conclusion that *o*-quinone imines such as **19**, **16**, and **22/24** catalyze the oxidation of the cysteinyl conjugates **6**, **7**, and **8**, respectively, from which they are derived.

The reaction pathways and products determined in this investigation relate specifically to the electrochemical oxidation of **1** in the presence of CySH at pH 7.4. It remains to be experimentally determined whether this oxidation chemistry mimics more biologically relevant reactions mediated by molecular oxygen or oxygen radicals. However, recent reports have demonstrated that the Fe^{2+}-promoted autoxidation, hydroxyl-radical- and peroxidase/H_2O_2-mediated[40] and electrochemical[13,41] oxidations of the related catecholamine DA are all potentiated by CySH and 5-*S*-CyS-DA and 2-*S*-CyS-DA are formed as initial products. Moreover, on the basis of the yields of these cysteinyl conjugates, compared to the DA consumed in the former chemical and enzymatic oxidation reactions and HPLC analysis of products[40] it might reasonably be concluded that 5-*S*-CyS-DA and 2-*S*-CyS-DA undergo further oxidations perhaps to dihydrobenzothiazines as predicted from more detailed electrochemical studies.[13,41] These apparent similarities between the electrochemical, chemical, and enzymatic oxidations of DA in the presence of CySH suggest that the present investigation might ultimately provide insights into the influence of CySH on the autoxidation and oxygen-radical-mediated oxidations of **1**. On the basis of this assumption it is possible to speculate about the potential neurobiological relevance of the results of this investigation. Thus, intraneuronal oxidation of **1** in the presence of CySH, both of which are cytoplasmic constituents, would be expected to lead to metabolites that are both lethal (**9** and **10**) and evoke a profound neurobehavioral response (**7**, **9**−**11**). Dihydrobenzothiazines **9** and **10** are relatively potent toxins in the brains of mice having LD_{50} values of 17.8 μg (66 nmol) and 23.4 μg (87 nmol), respectively. These LD_{50} values can be contrasted with that of the catecholaminergic neurotoxin 6-hydroxydopamine (6-OHDA), 134 μg (794 nmol),[42] a compound that has been considered as a possible endotoxin in PD.[43] Dihydrobenzothiazines **9**−**11** and cysteinyl conjugate **7** also evoke a profound neurobehavioral response in mice whereas 6-OHDA does not.[42] The mechanisms that underlie the *in vivo* neurobehavioral and/or lethal effects evoked by **7** and **9**−**11** remain to be elucidated. Furthermore, it must be stressed that at the current stage of this investigation there is no evidence that these compounds, other cysteinyl conjugates of **1**, or other dihydrobenzothiazines identified are either toxic toward noradrenergic or any other neurons or occur in the brain in neurodegenerative disorders. Nevertheless, it is known that **1** undergoes oxidation in the cytoplasm of noradrenergic LC cell bodies as evidenced by their pigmentation with neuromelanin polymer.[3,20] Futhermore, the results of this investigation tend to provide confirmation that LC cell bodies probably do not normally contain significant concentrations of CySH or GSH because these sulfhy-

dryl compounds would block the formation of neuromelanin pigment by scavenging *o*-quinone **2**.

The vulnerability of noradrenergic LC neurons to degeneration in PD might, similar to pigmented dopaminergic SN cells,[11,44] be linked to the fact that they sustain high basal levels of autoxidation of **1** and DA, respectively. The fact that both of these cell bodies degenerate in the Parkinsonian brain[11,12] and, at least in the SN, this is accompanied by a massive irreversible loss of GSH,[5,7,8] increased γ-GT activity,[10] and an increased 5-*S*-CyS-DA/DA ratio[9] all point to the idea that elevated cytoplasmic levels of CySH might be responsible for diverting the neuromelanin pathways forming, initially, cysteinyl conjugates of **1** (in the LC) and of DA (in the SN). Over the course of many years such a CySH-mediated diversion of these neuromelanin pathways would be expected to significantly reduce the amount of pigment deposited in these cell bodies and account for their apparent depigmentation in the Parkinsonian brain.[9] From a chemical perspective oxidation of cysteinyl conjugates of **1** should be inevitable under conditions where **1** is oxidized, *i.e.*, in the cytoplasm of pigmented LC neurons, to yield lethal dihydrobenzothiazines such as **9** and **10**. Work is currently in progress to determine whether cysteinyl conjugates of **1** or dihydrobenzothiazines that result from their facile oxidation (Table 1) are toxic toward noradrenergic or other LC neurons in order to provide support for the hypothesis that these compounds might include endotoxins that contribute to the neurodegeneration that occurs in PD.

Noradrenergic terminals also undergo profound degeneration in certain regions of the brain in AD[21] and as a consequence of transient cerebral ischemia.[22] Unlike noradrenergic cell bodies in the LC these terminals are rich in GSH and, presumably, its biosynthetic precursor CySH.[16] Furthermore, many lines of evidence indicate that in both AD[27−31] and transient cerebral ischemia[32,33] highly oxidizing conditions, perhaps mediated by oxygen radical species, develop in areas of the brain that include terminal regions of noradrenergic neurons, for example in the cortex.[24−26] Furthermore, following ischemia/reperfusion a significant loss of GSH occurs without a corresponding increase in GSSG levels.[34,35] This suggests that GSH is not lost as a result of its function as an oxygen radical scavenger or, in conjunction with glutathione peroxidase, detoxification of H_2O_2 because both of these processes should result in elevated levels of GSSG. Perhaps, therefore, the irreversible loss of GSH results in part from aberrant oxidation of **1** in noradrenergic terminals with resultant formation of glutathionyl and cysteinyl conjugates of the neurotransmitter followed by further oxidation to dihydrobenzothiazines by pathways similar to those conceptualized in Scheme 4. Such cysteinyl conjugates of **1** and/or resultant DHBTs might, therefore, represent endotoxins that contribute to the degeneration of noradrenergic terminals in selected regions of the AD brain and following an ischemic insult.

Experimental Section

(−)-Norepinephrine hydrochloride (NE·HCl) and L-cysteine (CySH) were obtained from Sigma (St. Louis, MO) and were used without additional purification. Trifluoroacetic acid (TFA) was obtained from Aldrich (Milwaukee, WI). HPLC grade acetonitrile was obtained from EM Science (Gibbstown, NJ). Voltammograms were obtained at a pyrolytic graphite electrode (PGE; Pfizer Minerals, Pigments and Metals Division, Easton, PA) having an approximate surface area of 6 mm^2. A conventional three-electrode voltammetric cell was used with a platinum wire counter electrode and a saturated calomel reference electrode (SCE). Cyclic voltammograms were obtained using a BAS-100A (Bioanalytical Systems, West Lafeyette, IN) electrochemical analyzer. All voltammograms were corrected for *iR* drop. Controlled potential electrolyses employed a Princeton Applied Research Corporation (Princeton, NJ) model 173 potentiostat. A three-compartment cell was used in which the working, counter, and reference electrode compartments were separated with Nafion membranes (type 117, DuPont Co., Wilmington, DE). The working electrode compartment had a capacity of 30 mL. The working electrode consisted of several plates of pyrolytic graphite having a total surface area of approximately 180 cm^2. The counter electrode was platinum gauze and the reference electrode a SCE. The solution in the working electrode compartment was continuously bubbled with a vigorous stream of N_2 and stirred with a Teflon-coated magnetic stirring bar. All potentials are referenced to the SCE at ambient temperature (22 ± 2 °C).

^{1}H NMR spectra were recorded on a Varian (Palo Alto, CA) XL-300 spectrometer. Low- and high-resolution fast atom bombardment mass spectrometry (FAB-MS) employed a VG Instruments (Manchester, UK) model ZAB-E spectrometer. Thermospray mass spectra were obtained with a Kratos (Manchester, UK) model 25/RFA instrument equipped with a thermospray source. Samples collected from preparative scale HPLC were injected into the thermospray source via a Rheodyne model 7125 loop injector equipped with a 2.0 mL loop. UV−visible spectra were recorded on a Hewlett-Packard (Palo Alto, CA) model 8452A diode array spectrophotometer.

High-performance liquid chromatography (HPLC) employed a Gilson (Middleton, WI) gradient system equipped with dual model 302 pumps (10 mL pump heads), a Rheodyne (Cotati, CA) model 7125 loop injector, and a Waters (Milford, MA) model 440 UV detector set at 254 nm. Two mobile phase solvents were employed. Solvent A was prepared by adding concentrated TFA to deionized water until the pH was 2.15. Solvent B was prepared by adding TFA to a mixture of 2 L of deionized water and 2 L of HPLC grade acetonitrile until the pH was 2.15. HPLC method I was employed to monitor the course of the electrochemical oxidation of NE in the presence of CySH and to purify reaction products and used a reversed phase column (Bakerbond C_{18}, 10 μm, 250 × 21.2 mm, P. J. Cobert Associates, St. Louis, MO) and the following gradient profile: 0−5 min, 100% solvent A; 5−40 min, linear gradient to 12% solvent B; 40−80 min, linear gradient to 50% solvent B; 80−85 min, linear gradient to 100% solvent B; 85−97 min, 100% solvent B. The flow rate was 7.0 mL min^{-1}. HPLC method II was used to isolate reaction products and employed a Bakerbond (J. T. Baker, Phillipsburg, NJ) reversed phase column (C_{18}, 10 μm particle size, 250 × 21.2 mm) and the following gradient profile: 0−60 min, linear gradient from 100% solvent A to 40% solvent B; 60−70 min, linear gradient to 100% solvent B; 70−82 min, 100% solvent B. The flow rate was 7.0 mL min^{-1}.

Animals. Outbred adult male mice of the HSD:ICR albino strain (Harlan Sprague-Dawley, Madison, WI) weighing 28−32 g were employed. Experimental animals were treated with test drugs dissolved in 5 μL of isotonic saline vehicle (0.9% NaCl in deionized water). Control animals were treated with 5 μL of vehicle alone. Animals were anesthetized with ether, and then drugs or vehicle were injected by means of a 10 μL microsyringe. Injections were performed freehand with the point of puncture being 3 mm anterior to the interaural line and 1 mm left lateral of the midline to a depth of 3 mm perpendicular to the scalp as described previously.[45] Animal procedures employed were approved by the Institutional Animal Care and Use Committee of the University of Oklahoma.

Oxidation Reaction Procedures. In a typical controlled potential electro-oxidation reaction **1**·HCl (3.1 mg; 0.5 mM) and CySH (3.65 mg; 1.0 mM) were dissolved in 30 mL of pH

7.4 phosphate buffer ($\mu = 0.2$). The resulting solution was electrolyzed at 70 mV for 30 min. Upon termination of the reaction the entire pale yellow solution was introduced onto the prepared reversed phase column via one of the HPLC pumps, and reactants and products were separated using method II. The solutions eluted under each of the major chromatographic peaks were collected individually and immediately frozen and stored at −80 °C. Following several repetitive experiments, the combined solutions containing each product were purified using HPLC method I. The solution of each product so obtained was then freeze-dried.

Electrochemical Synthesis of Cysteinyl Conjugates 6 and 7. **1**·HCl (6.2 mg; 1.0 mM) was dissolved in 30 mL of 0.1 M HCl and electrolyzed at 1.0 V for 30 min. The reaction solution changed from initially colorless to a bright yellow color characteristic of **2**. HPLC analysis (method I) revealed that ≥90% of **1** was converted to *o*-quinone **2**. Addition of CySH (7.3−14.6 mg; 2.0−4.0 mM) to the solution of **2** caused the bright yellow solution to rapidly become a very pale yellow color. The pH of the solution was adjusted to 8.0 with an aqueous solution of KOH and then to pH 2.15 with concentrated TFA. The total volume of solution was then directly pumped onto the preparative reversed phase column, and components were separated using an isochratic method that employed solvent A (flow rate: 7.0 mL min^{-1}). Cysteinyl conjugates **7** and **6** eluted at t_R values of 15 and 18 min, respectively. This procedure was repeated several times, the eluents containing **6** and **7** being collected individually. The combined solutions containing **6** and **7** were then freeze-dried. The resulting solid residues were dissolved in 2−10 mL of deionized water and adjusted to pH 2.15 with TFA and purified using the same isochratic HPLC method. The solutions containing **6** and **7** were then freeze-dried.

Spectroscopic evidence in support of the proposed structures of major products formed following oxidation of **1** in the presence of CySH are presented below. The assignments of various proton resonances observed in ^{1}H NMR spectra of products were based on comparisons with the spectra of **1** and CySH and were confirmed in all cases by two-dimensional correlated spectroscopy (COSY) experiments.

5-*S*-Cysteinylnorepinephrine (6). Compound **6** was isolated as a white solid. Anal. ($C_{11}H_{16}N_2O_5S$·$2CF_3COOH$) Calcd: C, 34.88; H, 3.49; N, 5.43; S, 6.20; F, 22.09. Found: C, 34.71; H, 3.50; N, 5.25; S, 6.45; F, 20.66. The UV spectrum of **6** at pH 7.4 exhibited bands, λ_{max}, nm (log ϵ_{max}, M^{-1} cm^{-1}), at 314 sh (3.13), 294 (3.46) and 254 (3.66). FAB-MS (glycerol/TFA matrix) gave m/e = 289.0875 (MH^+, 100, $C_{11}H_{17}N_2O_5$ S; calcd m/e = 289.0858). ^{1}H NMR (D_2O) gave δ 7.07 (d, $J_{2,6}$ = 2.1 Hz, 1H, C(2)-H), 6.93 (d, $J_{2,6}$ = 2.1 Hz, 1H, C(6)-H), 4.84 (dd, J = 8.4, 4.2 Hz, 1H, C(α)-H), 4.08 (dd, J = 6.3, 4.8 Hz, 1H, C(b)-H), 3.46 (dd, J = 15.0, 6.3 Hz, 1H, C(a)-H), 3.38 (dd, J = 15.0, 4.8 Hz, 1H, C(a)-H), 3.24 (dd, J = 13.2, 4.2 Hz, 1H, C(β)-H), 3.15 (dd, J = 13.2, 8.4 Hz, 1H, C(β)-H).

2-*S*-Cysteinylnorepinephrine (7). Compound **7** was isolated as a white solid. At pH 7.4 the UV spectrum exhibited bands at λ_{max}, nm (log ϵ_{max}, M^{-1} cm^{-1}), 318 sh (3.22), 298 (3.49), 256 (3.42) calculated as the 2TFA salt. FAB-MS (glycerol matrix) gave m/e = 289.0837 (MH^+, 30, $C_{11}H_{17}N_2O_5S$; calcd m/e = 289.0858). ^{1}H NMR (D_2O) gave δ 6.96 (s, 2H, C(5)-H and C(6)-H), 5.48 (dd, J = 8.7, 3.3 Hz, 1H, C(α)-H), 4.05 (dd, J = 6.9, 4.8 Hz, 1H, C(b)-H), 3.37 (dd, J = 14.7, 6.9 Hz, 1H, C(a)-H), 3.25 (dd, J = 14.7, 4.8 Hz, 1H, C(a)-H), 3.20 (dd, J = 13.2, 3.3 Hz, 1H, C(β)-H), 3.12 (dd, J = 13.2, 8.7 Hz, 1H, C(β)-H). ^{1}H NMR (CD_3OD) gave δ 7.07 (d, J = 8.4 Hz, 1H, C(5)-H), 6.97 (d, J = 8.4 Hz, 1H, C(6)-H), 5.48 (dd, J = 9.9, 3.3 Hz, 1H, C(α)-H), 3.94 (dd, J = 9.0, 4.2 Hz, 1H, C(b)-H), 3.41 (dd, J = 14.7, 4.2 Hz, 1H, C(a)-H), 3.25 (dd, J = 14.7, 9.0 Hz, 1H, C(a)-H), 3.19 (dd, J = 12.9, 3.3 Hz, 1H, C(β)-H), 3.03 (dd, J = 12.9, 9.9 Hz, 1H, C(β)-H).

2,5-Bi-*S*-cysteinylnorepinephrine (8). This compound was a white solid. At pH 7.4 λ_{max}, nm (log ϵ_{max}, M^{-1} cm^{-1}), 320 (3.56), 270 (3.80), 246 (4.10), calculated for the 2TFA salt. FAB-MS (glycerol/TFA matrix) gave m/e = 408.0895 (MH^+, 100, $C_{14}H_{22}N_3O_7S_2$; calcd m/e = 408.0899). ^{1}H NMR (D_2O) gave δ 7.25 (s, 1H, C(6)-H), 5.52 (dd, J = 8.4, 3.6 Hz, 1H, C(α)-H), 3.96 (t, J = 5.7 Hz, 1H, C(b)-H), 3.96 (t, J = 4.5 Hz, 1H, C(b′)-H), 3.51 (dd, J = 15.0, 5.7 Hz, 1H, C(a)-H), 3.50 (dd, J = 15.0, 5.7 Hz, 1H, C(a)-H), 3.34 (dd, J = 15.0, 4.5 Hz, 1H, C(a′)-H), 3.23 (dd, J = 13.2, 3.6 Hz, 1H, C(β)-H), 3.20 (dd, J = 15.0, 4.5 Hz, 1H, C(a′)-H), 3.12 (dd, J = 13.2, 8.4 Hz, 1H, C(β)-H).

7-(1-Hydroxy-2-aminoethyl)-3,4-dihydro-5-hydroxy-2*H*-1,4-benzothiazine-3-carboxylic Acid (9). Compound **9** was a very light yellow hygroscopic solid. Anal. ($C_{11}H_{14}N_2O_4S$·CF_3COOH). Calcd: C, 40.63; H, 3.91; N, 7.29; S, 8.33; F, 14.84. Found: C, 40.35; H, 3.84; N, 6.78; S, 8.14; F, 15.49. At pH 7.4, λ_{max}, nm (log ϵ_{max}, M^{-1} cm^{-1}), 304 (3.40), 238 (4.32). FAB-MS (3-nitrobenzyl alcohol matrix) gave m/e = 271.0753 (MH^+, 22, $C_{11}H_{15}N_2O_4S$; calcd m/e = 271.0753). ^{1}H NMR (Me_2SO-d_6) gave δ 9.70 (bs, 1H, C(5)-OH), 7.86 (bs, 3H, NH_3^+), 6.52 (d, J = 2.1 Hz, 1H, C(6)-H), 6.41 (d, J = 2.1 Hz, 1H, C(8)-H), 5.82 (bs, 1H, C(α)-OH), 5.31 (bs, 1H, N(4)-H), 4.52 (dd, J = 9.9, 3.0 Hz, 1H, C(α)-H), 4.35 (dd, J = 5.7, 3.3 Hz, 1H, C(3)-H), 3.15 (dd, J = 12.6, 3.3 Hz, 1H, C(2)-H), 3.07 (dd, J = 12.6, 5.7 Hz, 1H, C(2)-H), 2.90 (dd, J = 12.3, 3.0 Hz, 1H, C(β)-H), 2.74 (dd, J = 12.3, 9.9 Hz, 1H, C(β)-H). ^{1}H NMR (D_2O) gave δ 6.66 (s, 2H, C(6)-H and C(8)-H), 4.73 (dd, J = 8.7, 3.9 Hz, 1H C(α)-H), 4.66 (dd, J = 5.7, 3.6 Hz, 1H, C(3)-H), 3.37 (dd, J = 14.1, 3.6 Hz, 1H, C(2)-H), 3.31 (dd, J = 14.1, 5.7 Hz, 1H, C(2)-H), 3.11 (dd, J = 13.2, 3.9 Hz, 1H, C(β)-H), 2.98 (dd, J = 13.2, 8.7 Hz, 1H, C(β)-H).

8-(1-Hydroxy-2-aminoethyl)-3,4-dihydro-5-hydroxy-2*H*-1,4-benzothiazine-3-carboxylic Acid (10). Compound **10** was a very pale pink hygroscopic solid. At pH 7.4, λ_{max}, nm (log ϵ_{max}, M^{-1} cm^{-1}), 306 (3.39), 232 (4.33), calculated for the TFA salt. FAB-MS (3-nitrobenzyl alcohol matrix) gave m/e 271.0741 (MH^+, 30, $C_{11}H_{15}N_2O_4S$; calcd m/e = 271.0753). ^{1}H NMR (D_2O) gave δ 6.79 (d, J = 8.4 Hz, 1H, C(7)-H), 6.70 (d, J = 8.4 Hz, 1H, C(6)-H), 5.11 (dd, J = 8.1, 3.9 Hz, 1H, C(α)-H), 4.56 (dd, J = 4.2, 3.6 Hz, 1H, C(3)-H), 3.31 (dd, J = 13.2, 4.2 Hz, 1H, C(2)-H), 3.16 (dd, J = 13.2, 3.9 Hz, 1H, C(β)-H), 3.12 (dd, J = 13.2, 3.6 Hz, 1H, C(2)-H), 3.08 (dd, J = 13.2, 8.1 Hz, 1H, C(β)-H).

6-*S*-Cysteinyl-7-(1-hydroxy-2-aminoethyl)-3,4-dihydro-5-hydroxy-2*H*-1,4-benzothiazine-3-carboxylic Acid (11). Compound **11** was a very pale yellow solid. At pH 7.4, λ_{max}, nm (log ϵ_{max}, M^{-1} cm^{-1}), 324 (3.48), 282 sh (3.76), 252 (4.26), calculated for 2TFA salt. FAB-MS (thioglycerol/glycerol matrix) gave m/e = 390.0775 (MH^+, 26, $C_{14}H_{20}N_3O_6S_2$; calcd m/e = 390.0794). ^{1}H NMR (D_2O) gave δ 6.86 (s, 1H, C(8)-H), 5.41 (dd, J = 8.7, 3.6 Hz, 1H, C(α)-H), 4.61 (dd, J = 4.5, 3.6 Hz, 1H, C(3)-H), 3.94 (t, J = 5.7 Hz, 1H, C(b)-H), 3.32 (dd, J = 13.2, 4.5 Hz, 1H, C(2)-H), 3.26−3.19 (m, 3H, C(2)-H, C(a)-H_2), 3.16 (dd, J = 12.9, 3.6 Hz, 1H, C(β)-H), 3.13 (dd, J = 12.9, 8.7 Hz, 1H, C(β)-H).

6-*S*-Cysteinyl-8-(1-hydroxy-2-aminoethyl)-3,4-dihydro-5-hydroxy-2*H*-1,4-benzothiazine-3-carboxylic Acid (12). Compound **12** was a very pale yellow solid. Anal. ($C_{14}H_{19}N_3O_6S_2$·$2CF_3COOH$). Calcd: C, 35.01; H, 3.40; N, 6.81; S, 10.37; F, 18.48. Found: C, 35.13; H, 3.81; N, 6.75; S, 9.90; F, 17.61. At pH 7.4, λ_{max}, nm (log ϵ_{max}, M^{-1} cm^{-1}), 322 (3.44), 280 sh (3.74), 250 (4.30). FAB-MS (thioglycerol/glycerol matrix) gave m/e = 390.0792 (MH^+, 77, $C_{14}H_{20}N_3O_6S_2$; calcd m/e = 390.0794). ^{1}H NMR (D_2O) gave δ 7.02 (s, 1H, C(7)-H), 5.14 (dd, J = 7.8, 3.6 Hz, 1H, C(α)-H), 4.64 (t, J = 3.9 Hz, 1H, C(3)-H), 3.94 (t, J = 5.7 Hz, 1H, C(b)-H), 3.36 (dd, J = 13.2, 3.9 Hz, 1H, C(2)-H), 3.30 (d, J = 5.7 Hz, 2H, C(a)-H_2), 3.21 (dd, J = 13.2, 3.9 Hz, 1H, C(2)-H), 3.12 (dd, J =13.2, 7.8 Hz, 1H, C(β)-H), 3.11 (dd, J = 13.2, 3.6 Hz, 1H, C(β)-H).

6,7-Bi-*S*-cysteinyl-8-(1-hydroxy-2-aminoethyl)-3,4-dihydro-5-hydroxy-2*H*-1,4-benzothiazine-3-carboxylic Acid (13). Compound **13** was a very pale pink solid. At pH 7.4, λ_{max}, nm (log ϵ_{max}, M^{-1} cm^{-1}), 332 sh (3.58), 304 sh (3.64), 264 (4.29), calculated for the 2TFA salt. FAB-MS (thioglycerol/glycerol matrix) gave m/e = 509.0841 (MH^+, 100, $C_{17}H_{25}N_4O_8S_3$; calcd m/e = 509.0835). ^{1}H NMR (D_2O, 50 °C) gave δ 6.28 (dd, J = 10.2, 4.2 Hz, 1H, C(α)-H), 5.03 (t, J = 3.6 Hz, 1H, C(3)-H), 4.27 (t, J = 5.7 Hz, 1H, C(b)-H), 4.22 (t, J = 5.7 Hz, 1H, C(b′)-H), 4.17 (dd, J = 13.2, 10.2 Hz, 1H, C(β)-H), 3.70 (dd, J = 14.4, 5.7 Hz, 1H, C(a′)-H), 3.60 (dd, J = 13.5, 3.6 Hz, 1H, C(2)-H), 3.59 (dd, J = 14.4, 5.7 Hz, 1H, C(a′)-H), 3.59 (d, J = 5.7 Hz, 2H, C(a)-H_2), 3.51 (dd, J = 13.2, 4.2 Hz, 1H, C(β)-H), 3.17 (dd, J = 13.5, 3.6 Hz, 1H, C(2)-H).

Acknowledgment. This work was supported by National Institutes of Health Grant No. GM-32367. Additional support was provided by the Vice President for Research and the Research Council at the University of Oklahoma.

References

(1) Hornykiewicz, O.; Kish, S. J. Biochemical Pathophysiology of Parkinson's Disease. *Adv. Neurol.* **1986**, *45*, 19−34.
(2) Hornykiewicz, O. Aging and Neurotoxins as Causitive Factors in Idiopathic Parkinson's Disease−A Critical Analysis of Neurochemical Evidence. *Progr. Neuro-Psychopharmacol. Biol. Psychiatry* **1989**, *13*, 319−328.
(3) Graham, D. G. Oxidation Pathways for Catecholamines in the Genesis of Neuromelanin and Cytotoxic Quinones. *Mol. Pharmacol.* **1978**, *14*, 633−643.
(4) Rodgers, A. D.; Curzon, G. Melanin Formation by Human Brain In Vitro. *J. Neurochem.* **1975**, *24*, 1123−1129.
(5) Jenner, P.; Dexter, D. T.; Sian, J.; Schapira, A. H. V.; Marsden, C. D. Oxidative Stress as a Cause of Nigral Cell Death in Parkinson's Disease and Incidental Lewy Body Disease. *Ann. Neurol.* **1992**, *32*, S82-S87.
(6) Schapira, A. H. V.; Cooper, J. M.; Dexter, D.; Clark, J. B.; Jenner, P.; Marsden, C. D. Mitochondrial Complex I Deficiency in Parkinson's Disease. *J. Neurochem.* **1990**, *54*, 823−827.
(7) Riederer, P.; Sofic, E.; Rausch, W. D.; Schmidt, B.; Reynolds, G. P.; Jellinger, K.; Youdim, M. B. H. Transition Metals, Ferritin, Glutathione and Ascorbic Acid in Parkinsonian Brains. *J. Neurochem.* **1989**, *52*, 515−520.
(8) Sofic, E.; Lange, K. W.; Jellinger, K.; Riederer, P. Reduced and Oxidized Glutathione in the Substantia Nigra of Patients with Parkinson's Disease. *Neurosci. Lett.* **1992**, *142*, 128−130.
(9) Fornstedt, B.; Brun, A.; Rosengren, E.; Carlsson, A. The Apparent Autoxidation Rate of Catechols in Dopamine-Rich Regions of Substantia Nigra. *J. Neural Transm.* **1989**, *1* (P−D Sect.), 279−295.
(10) Sian, J.; Dexter, D. T.; Jenner, P.; Marsden, C. D. Glutathione−Related Enzymes in Brain in Basal Ganglia Disorders. *Br. J. Pharmacol.* (Suppl.) **1992**, *107*, 429P.
(11) Kastner, A.; Hirsch, E. C.; Lejeune, O.; Javoy-Agid, F.; Roscol, O.; Agid, Y. Is the Vulnerbility of Neurons in the Substantia Nigra of Patients with Parkinson's Disease Related to Their Neuromelanin Content? *J. Neurochem.* **1992**, *59*, 1080−1089.
(12) Mann, D. M. A.; Yates, P. O. Possible Role of Neuromelanin in the Pathogenesis of Parkinson's Disease. *Mech. Ageing Dev.* **1983**, *21*, 193−203.
(13) Zhang, F.; Dryhurst, G. Effects of L-Cysteine on the Oxidation Chemistry of Dopamine: New Reaction Pathways of Potential Relevance to Idiopathic Parkinson's Disease. *J. Med. Chem.* **1994**, *37*, 1084−1098.
(14) Orlowski, M.; Meister, A. The γ-Glutamyl Cycle. A Possible Transport System for Amino Acids. *Proc. Nat. Acad. Sci. U.S.A.* **1979**, *67*, 1248−1255.
(15) Meister, A. Glutathione: Metabolism and Function via the γ-Glutamyl Cycle. *Life Sci.* **1974**, *15*, 177−190.
(16) Slivka, A.; Mytilineou, C.; Cohen, G. Histochemical Evaluation of Glutathione in Brain. *Brain Res.* **1987**, *409*, 275−284.
(17) Carstam, R.; Brinck, C.; Hindemith-Augustsson, A.; Rorsman, H.; Rosengren, E. The Neuromelanin of the Human Substantia Nigra. *Biochim. Biophys. Acta* **1991**, *1097*, 152−160.
(18) Scatton, B.; Javoy-Agid, F.; Rouquier, L.; Dubois, B.; Agid, Y. Reduction in Cortical Dopamine, Noradrenaline, Serotonin and Their Metabolites in Parkinson's Disease. *Brain Res.* **1983**, *275*, 321−328.
(19) Farley, I. J.; Hornykiewicz, O. Noradrenaline in Subcortical Brain Regions of Patients with Parkinson's Disease and Control Subjects. In *Advances in Parkinsonism*; Birkmayer, W., Hornykiewicz, O., Eds.; Editiones Roche: Basel, Switzerland, 1976; pp 178−185.
(20) Tse, D. C. S.; McCreery, R. L.; Adams, R. N. Potential Oxidative Pathways of Brain Catecholamines. *J. Med. Chem.* **1976**, *19*, 37−40.
(21) Marcyniuk, B.; Mann, D. M. A.; Yates, P. O. The Topography of Cell Loss from Locus Coeruleus in Alzheimer's Disease. *J. Neurol. Sci.* **1986**, *76*, 335−345.
(22) Weinberger, J.; Cohen, G.; Nieves-Rosa, J. Nerve Terminal Damage in Cerebral Ischemia: Greater Susceptibility of Catecholamine Nerve Terminals Relative to Serotonergic Nerve Terminals. *Stroke* **1983**, *14*, 986−989.
(23) Jenner, P.; Schapira, A. H. V.; Marsden, C. D. New Insights into the Cause of Parkinson's Disease. *Neurology* **1992**, *42*, 2241−2250.
(24) Hardy, J. A.; Mann, D. M. A.; Wester, P.; Winblad, B. An Integrative Hypothesis Concerning the Pathogenesis and Progression of Alzheimer's Disease. *Neurobiol. Ageing* **1986**, *7*, 489−502.
(25) Mann, D. M. A. Neuropathological and Neurochemical Aspects of Alzheimer's Disease. In *Psychopharmacology of the Aging Nervous System*; Iversen, L. L., Iversen, S. D., Snyder, S., Eds.; Plenum Press: New York, 1988; pp 1−67.
(26) Hardy, J.; Adolfsson, R.; Alafuzoff, I.; Bucht, G.; Marcusson, J.; Nyberg, P.; Perdahl, E.; Wester, P.; Winblad, B. Transmitter Defecits in Alzheimer's Disease. *Neurochem. Int.* **1985**, *7*, 545−563.
(27) Smith, C. D.; Carney, J. M.; Starke-Reed, P. E.; Oliver, C. N.; Stadman, E. R.; Floyd, R. A.; Markesbery, W. R. Excess Brain Protein Oxidation and Enzyme Dysfunction in Normal Aging and in Alzheimer's Disease. *Proc. Nat. Acad. Sci. U.S.A.* **1991**, *88*, 10540−10543.
(28) Subbarao, K. V.; Richardson, J. S.; Ang, L. C. Autopsy Samples of Alzheimer Cortex Show Increased Peroxidation In Vitro. *J. Neurochem.* **1990**, *55*, 342−345.
(29) Zemlan, F. P.; Thienhaus, O. J.; Bosman, H. B. Superoxide Dismutase Activity in Alzheimer's Disease: A Possible Mechanism for Paired Helical Formation. *Brain Res.* **1989**, *476*, 160−162.
(30) Pappolla, M. A.; Omar, R. A.; Kim, K. S.; Robakis, N. K. Immunohistochemical Evidence of Antioxidant Stress in Alzheimer's Disease. *Am. J. Pathol.* **1992**, *140*, 621−628.
(31) Martins, R. N.; Harper, C. G.; Stokes, G. B.; Masters, C. L. Increased Cerebral Glucose-6-Phosphate Dehydrogenase Activity in Alzheimer's Disease May Reflect Oxidative Stress. *J. Neurochem.* **1986**, *46*, 1042−1045.
(32) Cao, W.; Carney, J. M.; Duchon, A.; Floyd, R. A.; Chevion, M. Oxygen Free Radical Involvement in Ischemia and Reperfusion Injury to the Brain. *Neurosci. Lett.* **1988**, *88*, 233−238.
(33) Oliver, C. N.; Starke-Reed, P. E.; Stadtman, E. R.; Liu, G. J.; Carney, J. M.; Floyd, R. A. Oxidative Damage to Brain Proteins, Loss of Glutamine Synthetase Activity and Production of Free Radicals During Ischemia/Reperfusion-Induced Injury to Gerbil Brain. *Proc. Nat. Acad. Sci. U.S.A.* **1990**, *87*, 5144−5147.
(34) Rehncrona, S.; Folbergrová, J.; Smith, D. B.; Siesjö, B. K. Influence of Complete and Pronounced Incomplete Cerebral Ischemia and Subsequent Recirculation on Cortical Concentrations of Oxidized and Reduced Glutathione in the Rat. *J. Neurochem.* **1980**, *34*, 477−486.
(35) Cooper, J. L.; Pulsinelli, W. A.; Duffy, T. E. Glutathione and Ascorbate During Ischemia and Postischemic Reperfusion in Rat Brain. *J. Neurochem.* **1980**, *35*, 1242−1245.
(36) Halliwell, B. Reactive Oxygen Species and the Central Nervous System. *J. Neurochem.* **1992**, *59*, 1609−1623.
(37) Young, T. E.; Babbitt, B. W. Electrochemical Study of the Oxidation of α-Methyldopamine, α-Methylnoradrenaline and Dopamine. *J. Org. Chem.* **1983**, *48*, 562−566.
(38) Pihel, K.; Schroeder, T. J.; Wightman, R. M. Rapid and Selective Cyclic Voltammetric Measurements of Epinephrine and Norepinephrine as a Method to Measure Secretion from Single Bovine Adrenal Medullary Cells. *Anal. Chem.* **1994**, *66*, 4532−4537.
(39) Dixon, W. J. The Up - and - Down Method for Small Samples. *J. Am. Stat. Assoc.* **1965**, *60*, 967−978.
(40) Palumbo, A.; d'Ischia, M.; Misuraca, G.; DeMartino, L.; Prota, G. Iron- and Peroxide-Dependent Conjugation of Dopamine with Cysteine: Oxidative Routes to the Novel Brain Metabolite 5-*S*-Cysteinyldopamine. *Biochim. Biophys. Acta* **1995**, *1245*, 255−261.
(41) Shen, X-M.; Dryhurst, G. Further Insights into the Influence of L-Cysteine on the Oxidation Chemistry of Dopamine: Reaction Pathways of Potential Relevance to Parkinson's Disease. *Chem. Res. Toxicol.* In press.
(42) Ma, S.; Lin, L.; Raghavan, R.; Cohenour, P.; Lin, P. Y. T.; Bennett, J.; Lewis, R. J.; Enwall, E.; Kostrzewa, R.; Lehr, R.; Blank, C. L. In Vivo and In Vitro Studies on the Neurotoxic Potential of 6-Hydroxydopamine Analogs. *J. Med. Chem.* **1995**, *38*, 4087−4097.
(43) Zigmond, M. J.; Hastings, T. G.; Abercrombie, E. D. Neurochemical Responses to 6-Hydroxydopamine and L-DOPA Therapy: Implications for Parkinson's Disease. *Ann. N. Y. Acad. Sci.* **1992**, *648*, 71−86.
(44) Hirsch, E.; Graybiel, A. M.; Agid, Y. Melanized Dopaminergic Neurons are Differentially Susceptible to Degeneration in Parkinson's Disease. *Nature* **1988**, *334*, 345−348.
(45) Wrona, M. Z.; Goyal, R. N.; Turk, D. J.; Blank, C. L.; Dryhurst, G. 5,5′-Dihydroxy-4,4′-Bitryptamine: A Potentially Aberrant Neurotoxic Metabolite of Serotonin. *J. Neurochem.* **1992**, 1392−1398.

JM960016T